High peak-power stretcher-free femtosecond fiber amplifier using passive spatio-temporal coherent combining

Louis Daniault, Marc Hanna, Dimitris N. Papadopoulos, Yoann Zaouter, Eric Mottay, Frédéric Druon, Patrick Georges

High peak-power stretcher-free femtosecond fiber amplifier using passive spatio-temporal coherent combining

L. Daniault,[1,*] M. Hanna,[1] D. N. Papadopoulos,[1,2] Y. Zaouter,[3] E. Mottay,[3] F. Druon,[1] and P. Georges[1]

[1]*Laboratoire Charles Fabry, Institut d'Optique, CNRS, Univ Paris-Sud, 2 Av. Augustin Fresnel, 91127 Palaiseau, France*

[2]*Laboratoire d'Utilisation des Lasers Intenses, CNRS, Ecole Polytechnique, CEA, Univ Pierre et Marie Curie, Palaiseau, France*

[3]*Amplitude Systèmes, 11 avenue de Canteranne, Cité de la Photonique, 33600 Pessac, France*

[*]*louis.daniault@institutoptique.fr*

Abstract: We report on the passive coherent combining of up to 8 temporally and spatially separated ultrashort pulses amplified in a stretcher-free ytterbium-doped fiber system. An initial femtosecond pulse is split into 4 temporal replicas using divided-pulse amplification, and subsequently divided in two counter-propagating beams in a Sagnac interferometer containing a fiber amplifier. The spatio-temporal distribution of the peak-power inside the amplifier allows the generation of record 3.1 µJ and 50 fs pulses at 1 MHz of repetition rate with 52 MW of peak-power from a stretcher-free fiber amplifier and without additional nonlinear post-compression stages.

OCIS codes: (060.2320) Fiber optics amplifiers and oscillators; (140.3298) Laser beam combining; (140.7090) Ultrafast lasers.

References and links

1. T. Eidam, S. Hanf, E. Seise, T. V. Andersen, T. Gabler, C. Wirth, T. Schreiber, J. Limpert, and A. Tünnermann, "Femtosecond fiber CPA system emitting 830 W average output power," Opt. Lett. **35**(2), 94–96 (2010).
2. F. Röser, T. Eidam, J. Rothhardt, O. Schmidt, D. N. Schimpf, J. Limpert, and A. Tünnermann, "Millijoule pulse energy high repetition rate femtosecond fiber chirped-pulse amplification system," Opt. Lett. **32**(24), 3495–3497 (2007).
3. F. Stutzki, F. Jansen, T. Eidam, A. Steinmetz, C. Jauregui, J. Limpert, and A. Tünnermann, "High average power large-pitch fiber amplifier with robust single-mode operation," Opt. Lett. **36**(5), 689–691 (2011).
4. E. Seise, A. Klenke, J. Limpert, and A. Tünnermann, "Coherent addition of fiber-amplified ultrashort laser pulses," Opt. Express **18**(26), 27827–27835 (2010).
5. L. Daniault, M. Hanna, L. Lombard, Y. Zaouter, E. Mottay, D. Goular, P. Bourdon, F. Druon, and P. Georges, "Coherent beam combining of two femtosecond fiber chirped-pulse amplifiers," Opt. Lett. **36**(5), 621–623 (2011).
6. A. Klenke, E. Seise, S. Demmler, J. Rothhardt, S. Breitkopf, J. Limpert, and A. Tünnermann, "Coherently-combined two channel femtosecond fiber CPA system producing 3 mJ pulse energy," Opt. Express **19**(24), 24280–24285 (2011).
7. L. Daniault, M. Hanna, D. N. Papadopoulos, Y. Zaouter, E. Mottay, F. Druon, and P. Georges, "Passive coherent beam combining of two femtosecond fiber chirped-pulse amplifiers," Opt. Lett. **36**(20), 4023–4025 (2011).
8. Y. Zaouter, L. Daniault, M. Hanna, D. N. Papadopoulos, F. Morin, C. Hönninger, F. Druon, E. Mottay, and P. Georges, "Passive coherent combination of two ultrafast rod type fiber chirped pulse amplifiers," Opt. Lett. **37**(9), 1460–1462 (2012).
9. S. Zhou, F. W. Wise, and D. G. Ouzounov, "Divided-pulse amplification of ultrashort pulses," Opt. Lett. **32**(7), 871–873 (2007).
10. L. J. Kong, L. M. Zhao, S. Lefrancois, D. G. Ouzounov, C. X. Yang, and F. W. Wise, "Generation of megawatt peak power picosecond pulses from a divided-pulse fiber amplifier," Opt. Lett. **37**(2), 253–255 (2012).
11. M. E. Fermann, V. I. Kruglov, B. C. Thomsen, J. M. Dudley, and J. D. Harvey, "Self-similar propagation and amplification of parabolic pulses in optical fibers," Phys. Rev. Lett. **84**(26), 6010–6013 (2000).

#169089 - $15.00 USD Received 23 May 2012; revised 27 Aug 2012; accepted 28 Aug 2012; published 6 Sep 2012

12. D. N. Papadopoulos, Y. Zaouter, M. Hanna, F. Druon, E. Mottay, E. Cormier, and P. Georges, "Generation of 63 fs 4.1 MW peak power pulses from a parabolic fiber amplifier operated beyond the gain bandwidth limit," Opt. Lett. **32**(17), 2520–2522 (2007).
13. Y. Zaouter, D. N. Papadopoulos, M. Hanna, J. Boullet, L. Huang, C. Aguergaray, F. Druon, E. Mottay, P. Georges, and E. Cormier, "Stretcher-free high energy nonlinear amplification of femtosecond pulses in rod-type fibers," Opt. Lett. **33**(2), 107–109 (2008).

1. Introduction

During the last decade, ytterbium-doped fiber amplifiers have been established as efficient femtosecond laser sources. Indeed, their geometry provides good thermal management and high optical-to-optical efficiency, allowing the generation of high repetition rate pulse trains at high average powers with nearly diffraction-limited beams [1]. The main drawback of these systems comes from the high peak power arising inside the fiber core that induces nonlinear effects and limits the achievable output pulse compressibility, energy, and therefore, peak power.

In general, the first detrimental effect that one faces in ultrafast fiber amplifiers is self-phase modulation (SPM), which depends on the optical intensity inside the fiber core. In recent years, large mode area (LMA) Yb-doped fiber amplifiers in combination with chirped pulse amplification (CPA) have permitted to lower SPM effects and reach higher peak-powers while maintaining good temporal pulse quality [2, 3]. Unfortunately, LMA fibers have limited core sizes, as transverse multimode operation inevitably appears with increasing core diameters. Additionally, the amplified beam can experience self-focusing (SF) inside the fiber at around 4 MW peak power and lead to optical damage. This drawback is a fundamental limitation of fiber amplifiers, as it does not depend on the core size.

Recently, coherent beam combining (CBC) has been used in the femtosecond regime to overcome these peak power related issues. The principle is the following: a single seed source is spatially split into several independent beams that are amplified in parallel under similar conditions and recombined using free space optics. The coherent addition of N beams eventually allows obtaining N times the energy available with a single fiber amplifier without cumulating nonlinearities.

The first experiments in the femtosecond regime [4, 5] report on the CBC of two femtosecond fiber CPA in a Mach-Zehnder interferometer with an active stabilization of their relative phase, involving phase detection schemes and feedback electronics. A subsequent high-energy experiment using this principle demonstrated the generation of 5.4 GW peak-power at 3 mJ pulse energy [6]. Passive CBC experiments in the femtosecond regime have also been recently demonstrated, exhibiting high robustness to environmental perturbations, no control electronics, and the ability to reach the multi-GW level [7, 8]. This has been achieved using a Sagnac interferometer (SI) that allows two counter-propagating beams to share the exact same optical path and be self-phase-matched.

Another coherent combining idea, denoted as divided-pulse amplification (DPA), acts in the temporal domain to split and recombine the pulses. It has been used to amplify picosecond pulses as a convenient substitute to chirped-pulse amplification [9, 10].

All femtosecond CBC experiments so far have been done with pulsewidths above 200 fs, because in quasi-linear CPA amplification regimes, the compressed pulsewidth is essentially determined by the seed pulse duration, the gain bandwidth available, and the gain narrowing effect. To overcome these limitations and generate shorter amplified pulses without nonlinear post-compression devices, stretcher-free architectures building upon the parabolic amplification regime [11] are possible, and take advantage of the combined action of SPM, dispersion, and gain in the amplifier to generate sub-100 fs pulses [12, 13]. So far, stretcher-free Yb-doped fiber amplifier performances have been limited by optical damage and SF to 1.25 µJ pulse energy and 16 MW output peak-powers [13].

We demonstrate in this paper that passive coherent combining concepts, both in time (DPA) and space (SI), can be implemented together in a stretcher-free architecture in order to

#169089 - $15.00 USD Received 23 May 2012; revised 27 Aug 2012; accepted 28 Aug 2012; published 6 Sep 2012

notably scale the energy and deliver 50 fs 3.1 µJ compressed pulses at 1 MHz repetition rate, exhibiting a peak power of 52 MW. These performances correspond to unprecedented operation of a fiber amplifier in the stretcher-free amplification regime. They also demonstrate that passive coherent combining both in the spatial and temporal domains is compatible with broadband spectra supporting sub-100 fs pulses, and B-integrals exceeding 20 rad.

2. Efficient spatio-temporal splitting and combining

In our experiment, the SI is made of a single fiber amplifier and a polarizing beam splitter that spatially divides and recombines two cross-polarized beams (Fig. 1 top). The seed is polarized at 45° so that it is equally distributed inside the interferometer. Furthermore, since our gain medium is polarization-dependent, a half-wave plate is inserted inside the loop to use the amplifier along the correct polarization for both counter-propagating beams. In such conditions, the Jones matrix of the SI is equivalent to a half-wave plate with neutral axes oriented at 45°, resulting in an output beam that exits through the seed path with unchanged polarization state. An optical isolator is inserted to extract it.

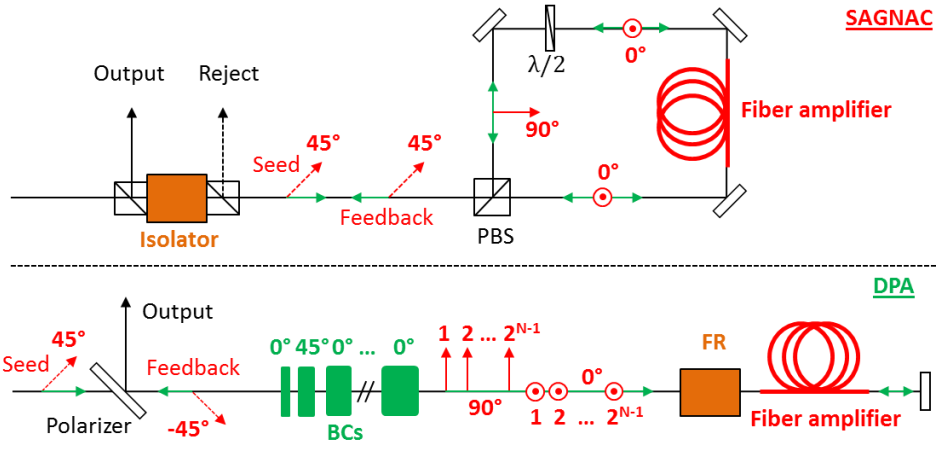

Fig. 1. Schematic representation of the spatial and temporal coherent combining techniques. Top: Sagnac geometry for spatial division. Bottom: DPA geometry for temporal division. PBS: Polarizing beam splitter; FR: Faraday rotator; BCs: birefringent crystals. The green arrows represent the direction of propagation while red arrows stand for the polarization states.

DPA consists in splitting and recombining ultrashort pulses in the temporal domain, thereby allowing a decrease of the optical peak power inside the amplifier. This can be achieved by using N consecutive highly birefringent crystals with increasing lengths and with their optical axes successively rotated by 45° [9] (Fig. 1 bottom). Each crystal divides a single pulse into two delayed cross-polarized replicas corresponding to the ordinary and extraordinary waves. The shortest crystal must generate a group-delay greater than the maximum pulse duration in the system to prevent interferences between the replicas. Then each additional crystal must have its length at least doubled in order to prevent any overlap between the duplicated patterns. Overall, a single seed pulse is split into 2^N time-delayed replicas with same power that are equally distributed into two cross polarizations. This usually forces the use of a polarization-insensitive amplifier. When a double-pass amplification configuration is used, the 2^N output pulses exit the amplifier through the seed path and go through the same crystals sequence but in the opposite direction. A Faraday rotator, inserted just before or inside the amplifier, allows all polarization of the amplified beam to be rotated by 90° with respect to the input beam, allowing all temporal replicas to experience the same total delay. This ensures an efficient temporal recombination. The final

#169089 - $15.00 USD Received 23 May 2012; revised 27 Aug 2012; accepted 28 Aug 2012; published 6 Sep 2012

unique output pulse is cross-polarized with respect to the original seed pulse and can therefore be extracted with a polarizer.

The SI and DPA architectures can be implemented together provided that all the time delayed replicas generated from the DPA are spatially split into the SI (Fig. 2 top). The time-delayed replicas created by the birefringent crystals are crossed-polarized. Thus, each replica can be separated into two counter-propagating beams into the SI if their input polarization states are oriented at 45° and −45° respectively. In this configuration, the SI geometry allows the use of DPA with polarization-dependent amplifiers, which is not achievable in a standard double-pass amplification configuration.

Figure 2 (top) shows the evolution of the polarization states of the replicas created at the last DPA stage through the system if the architectures shown in Fig. 1 are simply concatenated. The forward and backward propagation directions on the way in and out of the SI are separated to facilitate the reading. Since the SI behaves as a half-wave plate with neutral axes oriented at 45°, it introduces a phase shift of π between both input polarizations. On the way backward through the DPA crystals, the first temporal recombination step is carried out correctly, but results in a polarization state equal to the polarization state at the same point on the way forward. From this point on, the patterns accumulate delays instead of compensating them and temporal recombination is thus not possible.

To solve this issue, a quarter-wave plate with axes at 45° is inserted before the SI so that, together, they act as a neutral element for the polarization state and have no incidence on the replicas relative phase. The polarization in the system then follows the evolution shown in Fig. 2 (bottom). After complete temporal recombination, an optical isolator allows to extract the final pulse.

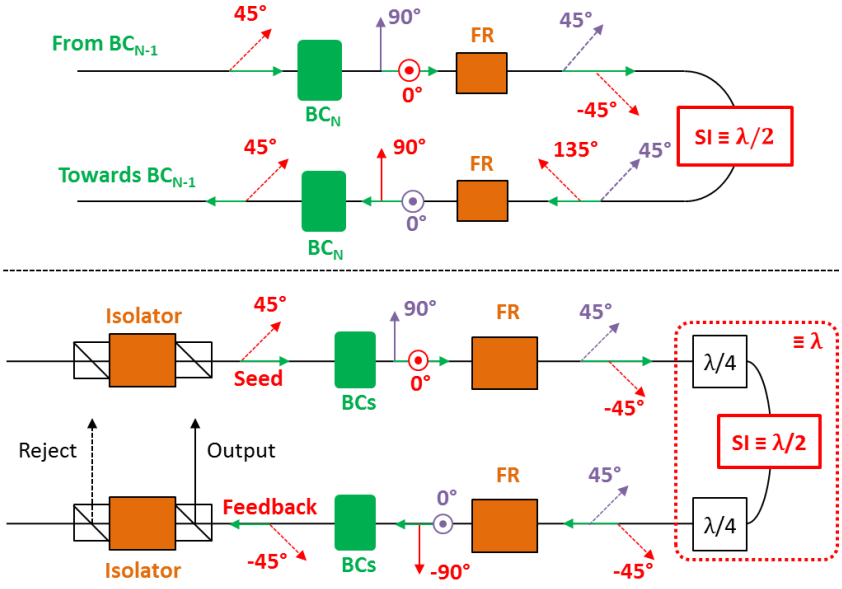

Fig. 2. Top: Evolution of the polarization state in the system if a quarter-wave plate is not inserted. Bottom: Schematic representation of the SI and DPA implemented together. FR: Faraday rotator. BC$_N$: birefringent crystal at position N in the sequence. The green arrows represent the direction of propagation while red and dash blue arrows stand for the polarization states.

Overall, 2×2^N spatio-temporal replicas are generated, thereby reducing the peak-power inside the fiber amplifier by the same factor. In our experiments, we create up to 8 sub-pulses with the SI and two temporal division steps.

#169089 - $15.00 USD Received 23 May 2012; revised 27 Aug 2012; accepted 28 Aug 2012; published 6 Sep 2012

3. Stretcher-free amplification and experimental results

The experimental setup is depicted in Fig. 3. It starts with an Yb^{3+}:KYW air-cooled commercially available oscillator (Mikan, Amplitude Systemes) delivering Fourier transform-limited sech-squared 200 fs pulses with 5 nm spectral bandwidth centered at 1030 nm. The repetition rate of the seed is 35 MHz and can be down-countered to 1 MHz by means of an acousto-optic modulator. The 35 MHz or 1 MHz pulse train is sent through two highly-birefringent YVO_4 crystals of 5 mm and 10 mm length that introduce group delays of 3.9 ps and 7.8 ps respectively. Half-wave plates precede both crystals in order to control the number of temporal divisions. This allows us to generate 1, 2 or 4 temporal replicas, corresponding to 0, 1 or 2 temporal divisions respectively. The beam then goes through a Faraday rotator (FR), a quarter-wave plate (QWP) properly oriented, and is equally divided inside the SI with the help of a half-wave plate. The interferometer includes a 2-m polarizing double-clad 40/200 µm Yb-doped fiber amplifier, which is pumped at both ends. The three devices together (FR + QWP + SI) allow the amplified beam going back toward the birefringent crystals to be rotated by 90° with respect to the input beam. This ensures both in-phase temporal recombination through the vanadate crystals and extraction of the final recombined output pulse with an optical isolator.

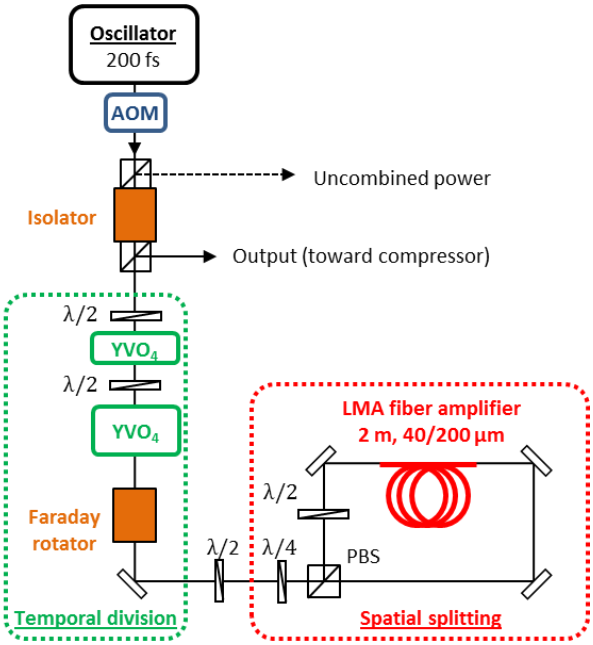

Fig. 3. Experimental setup of SI and DPA together with two birefringent vanadate crystals. AOM: acousto-optic modulator.

The DPA implementation involving birefringent crystals is only adapted to pulses in the picosecond range and below, because the group delays introduced by cm-length crystals are of the order of ~10 ps. In this experiment involving a stretcher-free architecture and a short fiber amplifier length, the interplay between SPM, dispersion, and gain results in an output pulsewidth that remains below 2 ps. The crystal-based DPA implementation is therefore well-suited to this amplification regime.

After extraction of the amplified beam by the isolator, it is directed toward a single-pass 1250 l/mm grating compressor adapted to compensate small chirp quantities. The single-pass compressor geometry induces a residual spatial-chirp of 200 µm which can be considered

#169089 - $15.00 USD Received 23 May 2012; revised 27 Aug 2012; accepted 28 Aug 2012; published 6 Sep 2012

negligible compared to the spot size of 4 mm and has low influence on the final diagnostics [12, 13]. In this configuration the compressor efficiency is 89%.

The combining efficiency is defined as the power extracted out of the seed path towards the compressor divided by the total power delivered by the amplifier, and is measured using both isolator ports. All the optical devices are chosen to handle large spectral width, in particular zero-order wave plates and broadband polarizing beam-splitters are used.

To ensure that the SI geometry can be used successfully at high nonlinearity levels with broadband spectra, we first operate without creating any temporal replicas. Indeed, in stretcher-free architectures where high nonlinearity levels are reached, the spectral shape and phase of the output pulses rapidly evolve with the injection conditions and pump powers. Differences in spectral contents for the two counter-propagating beams result in a decrease of the coherent combining efficiency. In addition, relative phase offsets between the two channels disturb the final polarization state coming out of the SI and prevent the amplified beam to be efficiently extracted through the optical isolator. Furthermore, if the DPA is activated, the temporal recombination is also affected by the non-perfect amplified polarization state, which further decreases the final peak-power. Thus, the SI needs to be very carefully adjusted and balanced and should exhibit the highest possible combining efficiencies before the DPA is activated.

In our experiments, temporal splitting and combining are easily performed efficiently. Indeed, because the pulse energy inside the amplifier is well below the saturation energy, temporally delayed replicas always see the same population inversion, are therefore identically amplified and exit with the same output spectral shape and phase, ensuring high efficiency for temporal recombination. The only constraint added by DPA is the need for temporally splitting the seed pulse into replicas of exact same power, which is easily achieved in our case. It has thus little influence on the combining efficiency if the SI is well-balanced.

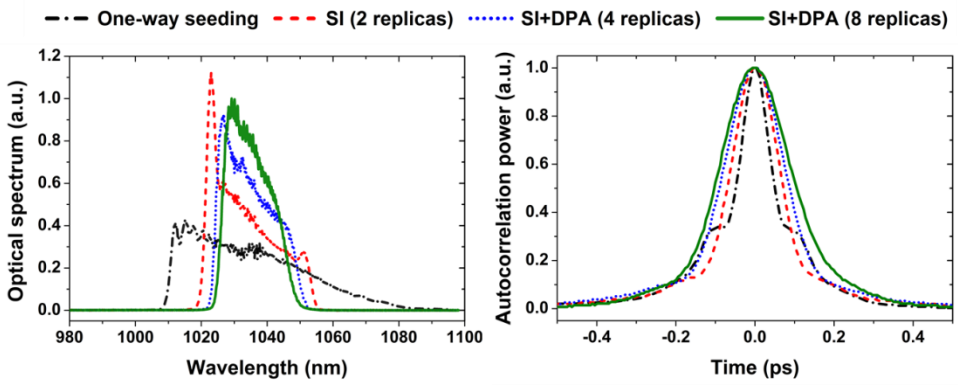

Fig. 4. Left: spectrum of 200 nJ pulses obtained with different numbers of spatial and temporal divisions. Right: Corresponding autocorrelations.

The setup is first operated at constant 200 nJ output compressed pulse energy, corresponding to 7 W average power at 35 MHz repetition rate. Figure 4 shows the output spectra and autocorrelations corresponding to an increasing number of spatial and temporal divisions. When seeding the fiber amplifier in a standard one-way amplification scheme, performed by coupling the whole seed power inside one interferometer arm only, the output spectrum is very broad, covering a wavelength range from 1010 nm to 1080 nm. Using the Sagnac geometry, the output spectral bandwidth is decreased compared to the single-pass configuration, demonstrating that the spatial division in the SI induces weaker SPM effects. After careful alignment, the SI exhibits a combining efficiency of 96%, which demonstrates its compatibility for wide spectral contents and high nonlinearity levels. As the DPA stages

#169089 - $15.00 USD Received 23 May 2012; revised 27 Aug 2012; accepted 28 Aug 2012; published 6 Sep 2012

are activated, creating successively 2 and 4 replicas, further spectral narrowing is observed as expected, while the SI combining efficiency remains over 95%.

The autocorrelation trace of the output beam at 200 nJ energy with 4 temporal divisions is shown with a large temporal window in Fig. 5 (left, black curve). Parasitic side pulses besides the main recombined pulse are barely observable, showing that the temporal recombination is almost perfect. Their overall contribution to the total energy is estimated to be less than 1%.

Finally, the setup is operated to deliver the highest possible peak-power before compression issues arise due to the accumulation of higher order spectral phase. The amplified pulse duration before compression is 1.7 ps at this energy level. With all temporal and spatial divisions activated, i.e. with 4 temporal replicas giving rise to 8 sub-pulses in the SI, 3.1 µJ pulse energy after compression is obtained at 1 MHz repetition rate. The SI combination efficiency is 89% and the B-integral is estimated to be 20 rad. At this pulse energy, it is not possible to align the SI alone since without temporal splitting, the peak-power inside the fiber would by far exceed the 4 MW SF threshold and damage the fiber. Among the 89% extracted energy, parasitic side pulses appear with non-negligible contribution, as shown in Fig. 5 (left). Indeed, at this nonlinearity level, the efficiency of the SI is much more sensitive to alignment, as it strongly depends on the injection quality and pumping conditions. It is thus experimentally challenging to reach a perfect balance in the SI, and small phase offsets appear between the two counter-propagating beams. This leads to a rotation of the spatially recombined beam polarization state. In turns, the non-ideal polarization state imparts an imperfect temporal recombination, creating small side pulses. We estimate that all the side pulses together contain 11% of the spatially combined energy. Overall, the spatio-temporal combination efficiency is 80% for the main central pulse. Since the system stability is mostly influenced by spatial aspects, we expect that a thorough opto-mechanical design of the system will result in an improvement of the overall stability at high energy level.

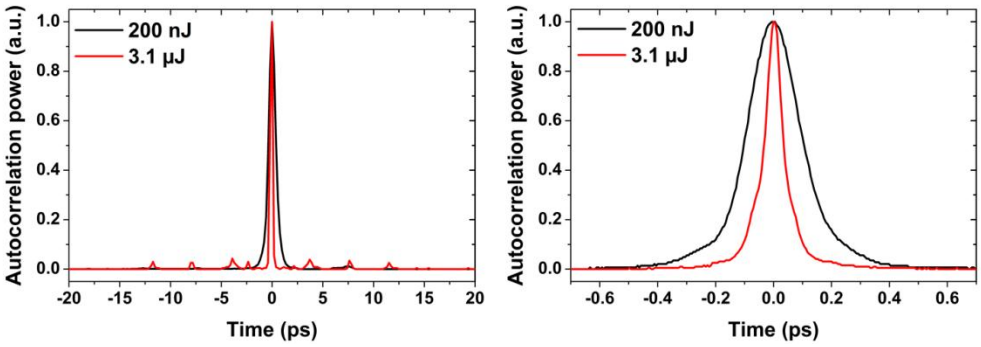

Fig. 5. Left: Large temporal range autocorrelations for 200 nJ and 3.1 µJ output energies using 4 DPA replicas and the Sagnac geometry together. Right: Corresponding short range autocorrelations.

The output pulses are characterized with a single-shot frequency-resolved optical gating (FROG) system, an independent autocorrelator, and a spectrometer. The retrieved intensity profile in the time domain is shown in Fig. 6 (left). It exhibits a pulse duration of 50 fs with a FROG error of 38.10^{-4} on a 512 × 512 grid. The independently measured autocorrelation trace shown in Fig. 5 (right) is in good agreement with the FROG-retrieved temporal profile. Taking into account that 80% of the overall output energy is in the main pulse, and the retrieved pulse shape, the peak power is calculated to be 52 MW. This represents a > 3-fold improvement in terms of achieved peak power despite using a gain medium having a mode field area almost 6 times smaller compared to the rod-type fiber previously used in [13]. The spectrum recorded at maximum energy is shown in Fig. 6 (right), and extends over 80 nm, with residual fringes due to the imperfect temporal recombination, and a characteristic peak

#169089 - $15.00 USD Received 23 May 2012; revised 27 Aug 2012; accepted 28 Aug 2012; published 6 Sep 2012

on the short-wavelength side related to the limited and asymmetric gain of the Yb-doped fiber.

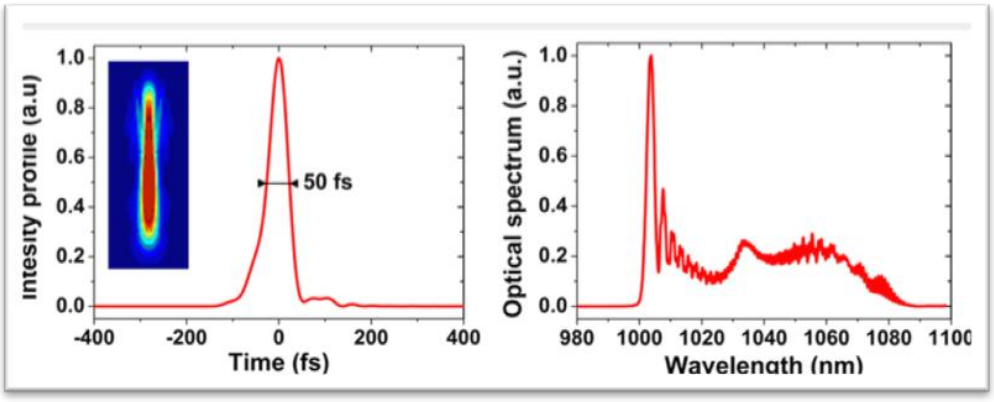

Fig. 6. Left: temporal pulse profile of the 3.1 µJ pulse retrieved from FROG measurement, along with the FROG trace (inset). Right: corresponding spectrum.

3. Conclusion

In conclusion, we have demonstrated that passive coherent beam combining can be used in a stretcher-free amplifier architecture to generate sub-100 fs pulses with high nonlinearity and broadband spectra, and can be scaled further by combining it with a temporal coherent combining concept. This work presents to our knowledge the shortest pulses ever obtained with a passive coherent combining scheme. A peak-power of 52 MW is obtained with a pulse duration of 50 fs which represent a > 3-fold improvement over the previously published state-of-the-art for such systems. We are convinced that this setup could be easily scaled in energy to reach output peak-powers of several hundreds of MW. Divided-pulse amplification has been demonstrated in the picosecond regime with five YVO_4 crystals [9], so that a factor-of-8 enhancement compared to these results is directly expected with a similar gain medium. Further scaling could also be expected from the use of larger core rod-type photonic crystal fibers. Such a simple fiber source that combines large peak power and very short pulse duration at high average power could be an ideal starting point for secondary radiations sources in the EUV using high-harmonic generation.

Acknowledgments

The authors acknowledge the financial support of Agence Nationale de la Recherche through the MultiFemto project.

#169089 - $15.00 USD Received 23 May 2012; revised 27 Aug 2012; accepted 28 Aug 2012; published 6 Sep 2012